ROYAL SOCIETY OF CHEMISTRY

EDGE ARTICLE

Check for updates

Subphthalocyanine capsules: molecular reactors for photoredox transformations of fullerenes†

Marta Moreno-Simoni,[a] Tomás Torres [ID] *[abc] and Gema de la Torre [ID] *[ab]

The internal cavity formed by a dimeric subphthalocyanine (SubPc) capsule (SubPc$_2$Pd$_3$, **2**), ensembled by coordination of pyridyl substituents in the monomeric SubPc **1** to Pd centers, has proved an optimal space for the complexation of C$_{60}$ fullerene. Taking advantage of the intense absorption of green light of the SubPc component at around 550 nm, we have tested different green-light induced photoredox addition reactions over the double bonds of guest C$_{60}$. Both addition of amine radicals, generated by reductive quenching of the excited state of **2** by aromatic trimethylsilylamines, and addition of trifluoroethyl radicals, obtained from oxidative quenching of the photosensitizer, have successfully taken place with good yields in the **2**:C$_{60}$ host:guest complex. On the other hand, both the photoredox reactions result in much lower yields when the monomeric pyridyl-SubPc is used as a photocatalyst, demonstrating that encapsulation results in a strong acceleration of the reaction. Importantly, this is the first example of the use of a confined microenvironment to trigger photoredox chemical transformations of fullerenes.
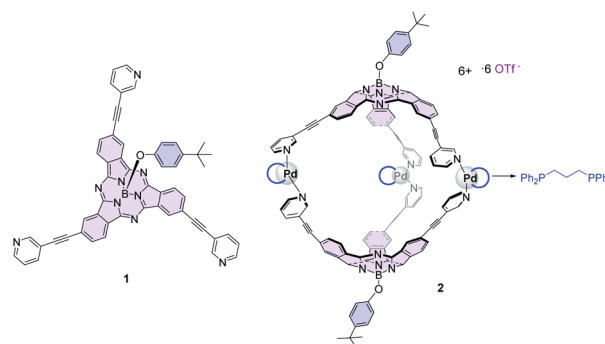
Introduction

The use of cage-like host systems as catalysts to perform reactions in confined microenvironments has become the centre of attention since the central cavity of molecular capsules is reminiscent of an enzyme-active site.[1] In particular, supramolecular coordination cages, easily prepared through modular approaches from metal ions and organic ligands, provide discrete microenvironments to bring the substrates together within the cavity, increasing the local concentration and triggering or accelerating chemical transformations.[2]

On the other hand, the use of chromophores that absorb visible light and trigger reactions after their excitation is central for the search of "green" synthetic methods.[3] The combination of the two fields, that is the formation of coordination cages by self-assembly of chromophores with photosensitizing abilities, offers powerful possibilities since it provides a local concentration of photoactive units surrounding a bound guest in a way that would not be possible in solution under normal conditions, affording an antenna effect in which excitation energy from several sources is directed to a single reaction site. Although there are examples in the literature of "antenna" cages performing as photocatalysts,[4,5] most of them are focused on the production of hydrogen or the generation of reactive oxygen species, and the realization of more complex photoredox transformations remains largely unexplored.

The development of chemical reactions under photoredox catalysis is a central research field that has allowed us to overcome issues, such as decomposition or the lack of control over the reaction, associated with the direct excitation of organic substrates with high energy UV-light.[6] Although Ir(III) and Ru(III) polypyridyl complexes are powerful visible-light catalysts for photoredox transformations, their low sustainability and potential toxicity have prompted the search for organic chromophores able to trigger electron transfer processes after photoexcitation with low-energy photon sources such as green or red light.[7] Phthalocyanines (Pcs) and their lower homologs subphthalocyanines (SubPcs) have been addressed as optimal

[a] Organic Chemistry Department, Universidad Autónoma de Madrid, Campus de Cantoblanco, 28049-Madrid, Spain

[b] Institute for Advanced Research in Chemical Sciences (IAdChem), Universidad Autónoma de Madrid, Campus de Cantoblanco, 28049-Madrid, Spain. E-mail: gema.delatorre@uam.es

[c] IMDEA-Nanociencia, C/Faraday 9, 28049-Madrid, Spain

† Electronic supplementary information (ESI) available: General experimental details, conditions for photoredox reactions, characterization of the new compounds and experiments for the elucidation of the mechanisms. See https://doi.org/10.1039/d2sc01931k

Fig. 1 Structure of Pd$_3$(SubPc)$_2$ cage **2** and its precursor **1**.

candidates for photoinduced electron transfer processes after excitation with visible light.[8] In particular, the bowl-shaped SubPcs (Fig. 1)[9] show intense transitions in the 550–630 nm region, and once photoexcited, they can act either as electron donors or acceptors as a function of the nature of the peripheral substituents. For that reason, they have been incorporated into multicomponent systems with other electroactive units to build photosynthetic models and advanced energy materials.[10] Electron-acceptor fullerenes are by far the most widely used units merged with SubPcs, particularly in a supramolecular manner, due to the shape complementarity between the concave face of SubPcs and the spherical π-surface of the fullerenes.[11] An outstanding illustration of this type of interaction is that exhibited by the SubPc-based coordination cage 2 reported by our group (Fig. 1), formed by Pd-directed dimerization of two C_3-symmetry SubPcs 1 endowed with three peripheral 3-pyridyl units,[12] which form stable 1 : 1 host–guest complexes with C_{60} and C_{70}.[13,14]

The recognition of fullerenes using metallo-organic cages constructed with other aromatic panels has also been accomplished by several authors.[15–25] The shape complementarity and space confinement in the host:guest complexes have a role in the reactivity of fullerenes, allowing reactions that do not proceed outside the cage,[15] or the control of the formation of different types of addition compounds.[19,26–29] However, the use of a confined microenvironment to trigger photoredox reactions over fullerenes has not yet been accomplished. In this regard, the use of SubPc cage 2 as an "antenna" pocket to induce photoredox transformations on fullerenes triggered by the surrounding SubPc excited states is a ground-breaking and conceptually innovative approach to obtain fullerene species that are not accessible by other means and can be of interest in areas such as solar energy conversion[10] or biomedicine.[30]

Despite their well-recognized abilities as photosensitizers for different applications, there are only a few examples in the literature of Pcs[31,32] and SubPcs[33] working as photoredox catalysts for organic transformations; in particular, fluorinated SubPcs have been recently tested as photocatalysts for radical additions of alkenes.[33] Our aim here is to take advantage of the strong interactions between the bowl-shaped SubPc units and the fullerene in the readily formed host:guest complexes in solution to trigger green-light induced photoredox addition reactions over the double bonds of C_{60}. As we will show in the following, confinement of C_{60} in the void space of 2 is essential to effectively perform the radical addition. Importantly, the internal dimensions of the cavity ($d_{Pd–Pd}$ = 18.4 Å; $d_{B–B}$ = 16.1 Å) may allow for co-binding of the reactive species.

Results and discussion

To prove that this SubPc cage can act as a molecular container for photoredox transformations, we have selected the addition of α-aminoalkyl radicals as a model reaction. Classically, reactions of C_{60} under high energy UV light irradiation with tertiary amines involve single electron transfer (SET) from the amines to the photoexcited C_{60}, leading to radicals that enable addition reactions to form different fullerene derivatives.[34–40] We have

selected diphenyl(trimethylsilylmethyl)amine[40] as a radical precursor to demonstrate the abilities of capsule 2 as a molecular photoreactor to accomplish addition reactions over fullerenes under benign green light illumination through SubPc-triggered SET processes. Importantly, to the best of our knowledge, this is the first time that a porphyrinoid cage works as a container for photocatalyzed fullerene derivatization. Then, with a protocol in hand, we have widened the applicability of our photocatalytic cage to other pioneering photocatalyzed radical additions over fullerenes.

Initially, the reaction was performed with 1.5 equivalents of diphenyl(trimethylsilylmethyl)amine 3a, using toluene (a good solvent for C_{60}) in the presence of 1% H_2O as a source of H^+ (necessary for the protonation of the intermediate anionic fulleroid, see the mechanism below) under continuous 530 nm irradiation, but in the absence of a photosensitizer. Under these conditions, as expected, no reaction took place due to the low energy of the light source (Table 1, entry 1). Before starting the photocatalyzed experiments, the stability of SubPc 1 and cage 2[14] under green light LED irradiation for periods of up to 12 h was confirmed. Then, the photocatalyzed reaction was set using 1 equivalent of SubPc cage 2 to ensure maximum complexation of C_{60} in the interior (Table 1, entry 2). After 9 h of reaction at rt, a fullerene derivative was isolated in 83% yield, with ^{1}H-NMR and MS features that match with the addition of the α-diphenylaminomethylene radical (Fig. S1†). The 1,2-addition pattern of 4a was confirmed in the UV-vis spectrum, which shows a weak transition at 435 nm, characteristic for this type of adduct (Fig. S4†).

To determine if encapsulation is necessary for the reaction to proceed, SubPc 1 was tested as a photosensitizer (Table 1, entry 3). In this case, the addition product 4a was isolated in only 20% yield, which evidences the benefits of performing the reaction

Table 1 Optimization of the photoredox reaction of C_{60} with 3a in the SubPc cage^a

Entry	PS (equiv.)	Time (h)	Solvent	Yield
1	—	9	Toluene	—
2	2 (1.0)	9	Toluene	83%
3	1 (1.0)	9	Toluene	20%
4	2 (1.0)	9	DCM	87%
5^b	2 (1.0)	9	DCM	75%
6	2 (0.1)	9	DCM	31%
7	2 (1.0)	6	DCM	86%
8	2 (1.0)	3	DCM	72%
9	2 (1.0)	1.5	DCM	43%

^{a} PS = Photosensitizer. Conditions: C_{60} (0.003 mmol) 0.08 M, 3a (1.5 equiv.), at rt with irradiation by a 530 nm LED under Ar. Isolated yields of 4a. ^{b} 2 equiv. of 3a.
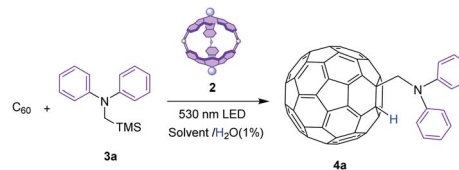
in a confined space. Another important conclusion from this experiment is that the SubPc chromophore is responsible for triggering the photoredox reaction, ruling out the possibility of Pd(ɪɪ) behaving as catalytic centers. The only role of the metals is to bind the two SubPc units, although they also provoke a slight deactivation of the SubPc excited state (Fig. S2†), which does not otherwise reduce the photocatalytic activity of the cage.

To maximize the formation of the host–guest complex, we decided to change the reaction solvent to CH_2Cl_2, which is a poorer solvent for C_{60}. In fact, binding constants have been derived from UV-vis titration experiments with values as high as 4.7×10^5 M^{-1} (Fig. S11†). It is also important to mention here that although SubPc **1** interacts with C_{60} also in CH_2Cl_2, binding isotherms (Fig. S12†) reveal poor fitting and lower binding constants (*ca.* 10^4). This finding points out again the importance of the confined microenvironment for the reaction to take place smoothly, which could probably be a consequence of the increased local concentration of the reactants inside the cavity and/or a larger antenna effect caused by the two SubPc units in cage **2**.

Then, when the reaction was carried out in CH_2Cl_2 (entry 4), slightly higher yields of the isolated product (*i.e.*, 87%) were achieved. However, when the amount of amine **3a** was increased (entry 5), the yield of **4a** decreased, while other products appeared in the reaction mixture, showing molecular peaks in the mass spectra that correspond with double additions of the amine radical to the fullerene (Fig. S3†). Finally, the amount of **2** was reduced to 10 mol% with respect to C_{60}, but the yield of **4a** dropped to 31% (entry 6) which may be probably caused by the competitive inhibition by the product, *i.e.*, involvement of the resulting adduct **4a** in the host–guest equilibrium with the SubPc cage, which hampers the complexation of pristine fullerene, as in previous examples of temperature-promoted reaction of fullerenes in metallocages.[19,26–29] To demonstrate the inhibition by the product, we accomplished the assessment of the binding constants for the host:guest complex formation between **4a** and **2**. However, the insolubility of the adduct in CH_2Cl_2 (and also in toluene) prevented the realization of the experiments. Yet, it must be considered that this insolubility may be the driving force that pushes the adduct **4a** to remain in the SubPc capsule (*i.e.*, solvophobic effect). Importantly, although optimal results are achieved using 1 equiv. of the cage, 80% of the initial amount of **2** is recovered after treatment of the reactions, and it performed with the same efficiency in further

Table 2 Photoredox reaction of C_{60} with amines **3b–h** in the SubPc cage[a]

| 3b → 4b (71%) | 3c → 4c (74%) | 3d → 4d (68%) |
| 3e → 4e (0%) | 3f → 4f (65%) | 3g → 4g (52%)   3h → 4h (0%) |
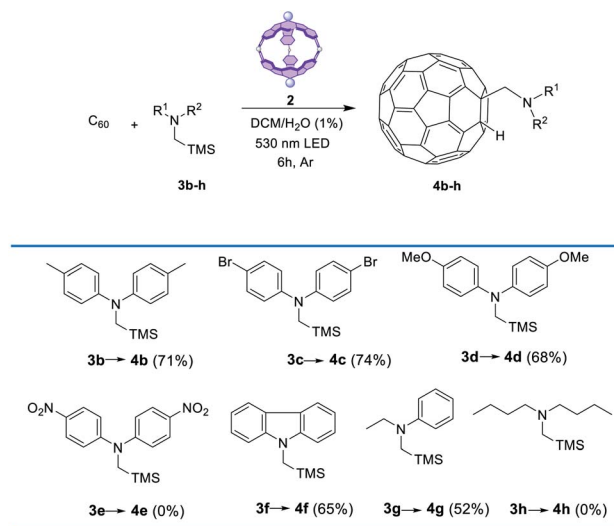
[a] Conditions: C_{60} (0.003 mmol) 0.08 M, **3b–h** (1.5 equiv.), **2** (1 equiv.), at rt with irradiation by a 530 nm LED under Ar.

photoredox cycles. Eventually, an assessment of the reaction kinetics was performed (entries 4 and 7–9), measuring the yields of **4a** at different reaction times. As shown in Fig. 2, the reaction undergoes a strong acceleration in the first three hours, and then it slows down until a plateau is reached (*i.e.*, 6 h) after which the yield remains stable.

With a general protocol in place (CH_2Cl_2, 1 equiv. of **2**, 1.5 equiv. of amine *vs.* C_{60} and 6 h green-light irradiation at rt) we searched to broaden the scope of the reaction using different α-silylamines (Table 2). For the reactions with amines functionalized with strong or moderate electron donors (**3b–d**), the yields of the corresponding adducts **4b–e** were moderately lower than those of the model reaction. Similar yields were achieved with other types of electron-rich aromatic amines (**3f**). Interestingly, the reaction with the NO_2- functionalized silylamine **3e** did not work out, which can be rationalized considering the proposed mechanism (see below). Finally, group substitution of one phenyl ring with an alkyl radical (amine **3g**) led to yield reduction (*i.e.*, 52%), while the use of dialkylamine **3h** resulted
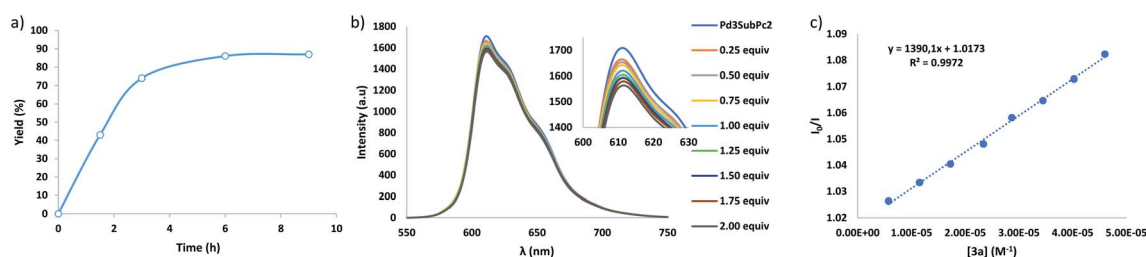

Fig. 2 (a) Kinetic profile for the conversion of C_{60} in **4a**; (b) fluorescence quenching of **2** (2.14×10^{-5} M in CH_2Cl_2) upon addition of increasing amounts of **3a**; (c) plot of the fluorescence quenching of **2** *versus* [**3a**] and determination of the Stern–Volmer constant ($I/I_0 = 1 + K_{SV}\cdot x$).

in full inactivation of the process. Characterization of **4b–g** is provided in the ESI (Fig. S7–S10)†.

With a general protocol in place, the next step was the elucidation of the mechanism using the model reaction. Previous photophysical studies on $C_{60} \subset 2$ complexes concluded that after excitation of the SubPc, no SET to C_{60} was observed but energy transfer occurred,[14] which excludes the oxidative quenching of **2** by C_{60}. Nevertheless, the formation of a radical species in the herein described transformation is confirmed by the absence of reaction when it was carried out in the presence of 2 equiv. of 2,2,6,6-tetramethylpiperidin-1-oxyl (TEMPO) radical scavenger, which yielded the diphenylmethylamine-TEMPO product by radical coupling (Fig. S13†).[41] Therefore, the formation of the diphenylmethyl-amine radical species could be rationalized by initial SET from **3a** to the photoexcited SubPc units in **2**. This hypothesis was supported by Stern–Volmer fluorescence quenching experiments, which evidence that the amine **3a** quenches the excited state of **2** (Fig. 2). Considering the high degree of occupancy of cage **2** with C_{60} under the reaction conditions, we have also performed Stern–Volmer experiments using a $C_{60} \subset 2$ complex synthesized by assembly of the cage in the presence of fullerene.[14] As expected, the results derive a similar K_{SV} (Fig. S15†).

To confirm the deactivation of the excited state of the cage by the amine, a reaction was set with a 1 : 1 mixture of **2** and **3a** under green LED photoirradiation for 6 h, in the absence of C_{60}, which led to the conversion of the trimethylsilylamine to Me$_3$-SiOH (Fig. S9†). This result is rationalized by the reductive quenching of the photoexcited SubPc units by **3a**, leading to the radical cation form of the amine that suffers desilylation assisted by water to give an α-diphenylaminomethyl radical (Fig. 3). In an additional control reaction, a solution of **3a** in DCM/H$_2$O was irradiated, which provided the amine unaltered (Fig. S9†).

The reductive quenching of **2** by diphenyl(-trimethylsilylmethyl) amine is plausible considering that the excited state reduction potential of **2** (0.771 eV *vs.* SCE,

calculated from $E^*_{red} = E_{red}(2/2^-) + E_{00}$) exceeds the oxidation potential of **3a** (0.471 eV *vs.* SCE) (Fig. S16 and 17†). Please note that the oxidation potential of amine **3e** is 1.07 eV (Fig. S17†), which explains why the reaction with **3e** failed to proceed. All these calculations are done considering the singlet as the involved excited state in the photoredox reaction, since the triplet energy (1.45 eV) is too low to be involved in the oxidation of the amine.

Then, the more plausible pathway is that after reductive quenching, addition of the α-aminomethyl radical to the fullerene gives a fulleroid radical, which can be further reduced by SET from the one-electron reduced form of **2** (**2$^-$**) to give an anionic fullerene that is further protonated (Fig. 3). This last step of the catalytic cycle is supported by the fact that no reaction occurs in the absence of water. Moreover, the signal of the added H does not appear in the ^{1}H-NMR spectrum when the reaction is carried out in DCM/D$_2$O mixtures (Fig. S19†). Importantly, other pathways derived from the C_{60} excited state are excluded since the reaction between C_{60} and amine **3a** under green LED irradiation does not take place in the absence of a photocatalyst (Table 1, entry 1).

After these outstanding results, we aimed to prove that SubPc cage **2** is a versatile molecular container for other types of photoredox reactions with fullerenes. Considering the increasing interest in fluoroalkyl groups for several applications, including medicinal chemistry,[30] fluoroalkylation reactions over fullerenes are relevant targets of research.[42] Radical addition of fluoroalkyl radicals to fullerenes has been achieved by thermal or photochemical decomposition of fluoroalkyl iodides. However, to the best of our knowledge, the photocatalyzed fluoroalkyl addition using low-energy light sources has not been undertaken yet.

Among the different photocatalyzed fluoroalkylation reactions, we have selected the straightforward trifluoroethylation with CF$_3$CH$_2$I as a model reaction. The photocatalyzed reaction of fluorinated alkyl iodides with alkenes can yield atom transfer radical additions (ATRA), where the final alkene bears the two functionalities (*i.e.*, CF$_3$ and I),[43] or hydrofluoralkylated compounds.[44] Then, we have accomplished the photocatalytic activation of CF$_3$CH$_2$I by our cage **2** to generate radicals[45] that subsequently react with fullerene to give **5a** or **5b** (Table 2).

As the high reduction potential of CF$_3$CH$_2$I (-1.4 eV *vs.* SCE) rules out the possibility of forming the trifluoromethylene radical by oxidative quenching of photoexcited **2** (excited state oxidation potential of SubPc cage **2** is -0.92 eV), the addition of sacrificial reductants seems necessary. After testing different additives (see Table 3), we found that the addition of 1 equiv. of PPh$_3$[46] (entry 3) resulted in the formation of hydro-trifluoroethylated fullerene **5b** (Fig. S13†) in 65% yield. The formation of this product requires hydrogen-atom transfer (HAT) from a hydrogen donor, most likely the solvent (CH$_2$Cl$_2$). Noteworthily, the formation of **5a** was not detected under any of the tested conditions, probably because the incorporation of the iodide requires oxidation of the fullerene radical that results from the trifluoromethylene addition into a carbocation, and this step requires a strongly oxidative catalytic species (see the mechanism below). As in previous hydroaminations, the
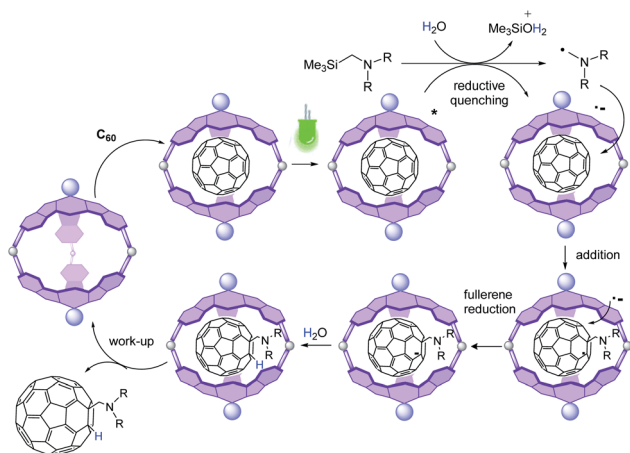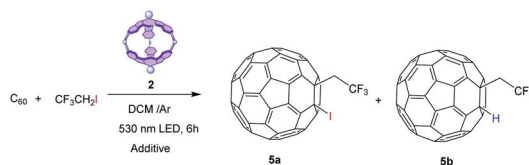

Fig. 3 Postulated photoredox mechanism for the conversion of C_{60} to **4a**.

Table 3 Photocatalyzed trifluoroalkylation of C_{60}[a]

Entry	PS (equiv.)	Additive (equiv.)	Yield (5a)	Yield (5b)
1	**2** (1.0)	Lutidine (1.0)	—	—
2	**2** (1.0)	Sodium ascorbate/NaOAc (1.0)	—	—
3	**2** (1.0)	PPh₃ (1.0)	—	65%
4	**2** (0.2)	PPh₃ (1.0)	—	27%
5	**1** (1.0)	PPh₃ (1.0)	—	9%
6	—	PPh₃ (1.0)	—	—

[a] PS = Photosensitizer. Conditions: C_{60} (0.003 mmol) 0.08 M, CF_3CH_2I (1.5 equiv.) at rt with irradiation by a 530 nm LED under an Ar atmosphere. Isolated yields of **5a** and **5b**.

reaction performed more efficiently when using equimolar amounts of SubPc cage **2** rather than catalytic amounts (entry 4), but it is important to remark that 75% of **2** was recovered after treatment of the reaction, and it proved effective in further photoredox reactions. Again, the need of the molecular cavity for the reaction to proceed efficiently was proved, as the reaction yield dropped to 9% when SubPc **1** was used as the catalyst. Finally, the reaction performed in the absence of a SubPc derivative was ineffective, which demonstrates that the photocatalyst is necessary for the reaction to take place (entry 6).

In subsequent mechanistic investigations, we found that the addition of TEMPO completely inhibited the reaction, confirming the radical character of the reaction (see Fig. S22† for

the ^{19}F-NMR spectrum of the CF_3CH_2-TEMPO coupling product). Stern–Volmer experiments revealed that neither CF_3CH_2I nor PPh₃ alone quenched the excited state of **2** (Fig. 4). However, fluorescence titration with an equimolecular mixture of CF_3CH_2I and PPh₃ yielded quenching of the emission of **2**, with a Stern–Volmer constant of 2995 M^{-1}. This finding implies that coordination of phosphine to CF_3CH_2I may lower the reduction potential of the haloalkane.‡ Halogen bonding between the iodine atom in CF_3CH_2I and the Lewis base PPh₃ is plausible,[47] because the "sigma-hole" of the iodine atom is enhanced by the three electron-withdrawing fluorines. From this result, it could be derived that after excitation of **2**, an oxidative quenching is caused by the CF_3CH_2I–PPh₃ complex
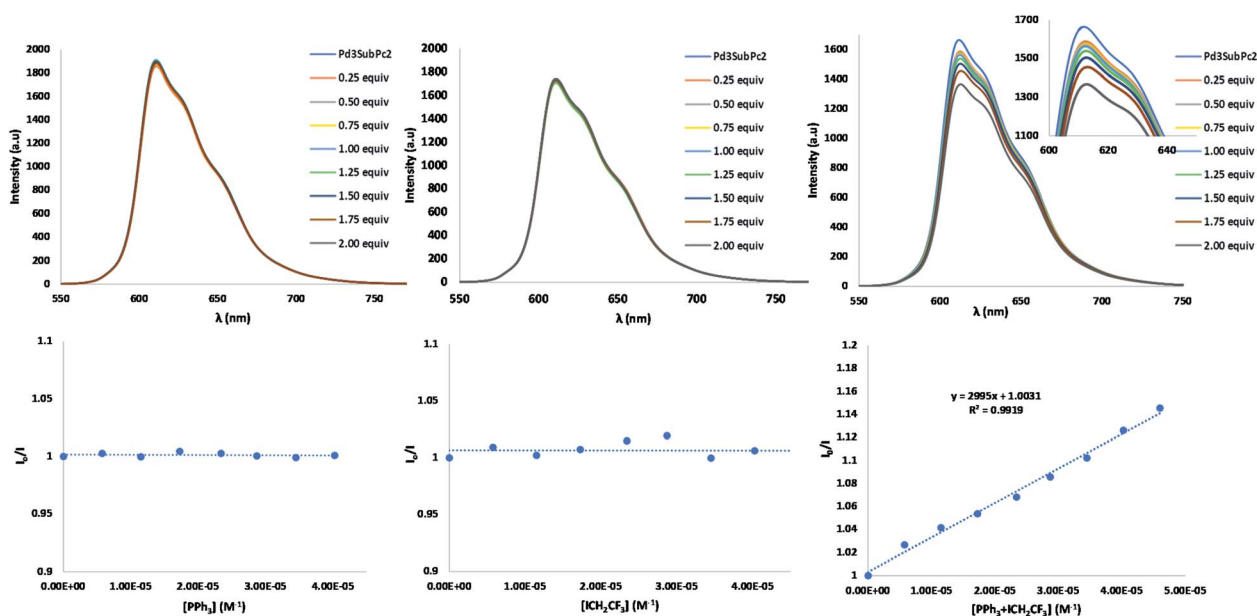

Fig. 4 Fluorescence quenching and plot of the quenching of **2** (2.14×10^{-5} M in CH_2Cl_2) *versus*: [PPh₃], left column; [ICH₂CF₃], middle column; and [PPh₃ + ICH₂CF₃], right column. Determination of the Stern–Volmer constant ($I/I_0 = 1 + K_{SV} \cdot x$).
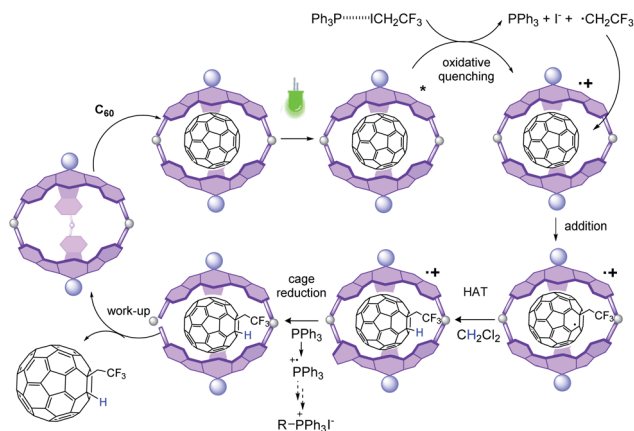
Fig. 5 Postulated photoredox mechanism for the conversion of C_{60} to **5b**.

(Fig. 5). The resulting radical anionic species could split into PPh_3, iodide and the trifluoroalkyl radical, whose addition to fullerene results in the formation of the trifluoroethylated fullerene radical. The oxidized form **2** (**2+**) does not appear to oxidize this radical to its carbocationic form; instead, in the absence of an extra hydrogen source, CH_2Cl_2 solvent can act as a hydrogen donor for subsequent HAT to fullerene. To confirm this hypothesis, the reaction was performed in CD_2Cl_2, which provided the deuterated analog **5b** (Fig. S24†). Reduction of the oxidized form of the SubPc photocatalytic cage **2** should be completed by PPh_3 ($E^{1/2}_{ox} = 0.98$ vs. SCE), which also plays the role of a sacrificial reductant.

Conclusions

All the previous results indicate that SubPc capsule **2** is a powerful photosensitizer to trigger additions of (diaryl) methylamine and trifluoroethyl radicals to C_{60} fullerene. Taking advantage of the ready formation of host:guest complexes between **2** and C_{60} fullerene in CH_2Cl_2, the capsule behaves as a molecular photoreactor. Very remarkable is the versatility of the SubPc cage, which can initiate photoredox processes in the form of reductive or oxidative quenching. Probably due to the strong interaction between the C_{60} addition products and the SubPc cage, which do not allow a rapid exchange of the product by the pristine C_{60} substrate, equimolar amounts of **2** are necessary to maximize the yields. Despite that, the SubPc cage is recovered to a large extent after the reactions and can be used in further cycles. Undoubtedly, the reactions strongly benefit from being performed in the confined space, because when monomeric SubPc is used as a photocatalyst, the yields dropped considerably. This work is conceived as a proof-of-concept, demonstrating the capabilities of SubPc cages as molecular photoreactors, and setting the basis for the search for other "eco-friendly" green light-induced, photoredox transformations over fullerene species, which can provide interesting, functionalized fullerenes with applications in energy conversion schemes or biomedicine.

Data availability

All data were given in ESI.†

Author contributions

M. M.-S. performed all the the experimental work. T. T, coordinated the work. G. T. originated the central idea, coordinated the work, and analyzed the experimental data. The manuscript was written through contributions of all authors.

Conflicts of interest

There are no conflicts to declare.

Acknowledgements

Notes and references

‡ In a control reaction, it was checked that PPh_3 and ICH_2CF_3 did not form the corresponding phosphonium derivative under these conditions, ruling out its participation in the reaction.

1 C. J. Brown, F. D. Toste, R. G. Bergman and K. N. Raymond, *Chem. Rev.*, 2015, **115**, 3012–3035.

2 Y. Xue, X. Hang, J. Ding, B. Li, R. Zhu, H. Pang and Q. Xu, *Coord. Chem. Rev.*, 2021, **430**, 213656.

3 C. R. J. Stephenson, T. P. Yoon and D. W. C. MacMillan, *Visible Light Photocatalysis in Organic Chemistry*, Wiley-VCH, Weinheim, Germany 2018.

4 T. Comerford, E. Zysman-Colman and M. D. Ward, in *Reactivity in Confined Spaces*, ed., R. S. Forgan and G. O Lloyd, The Royal Society of Chemistry, 2021, pp. 70–107.

5 H. Y. Lin, L. Y. Zhou and L. Xu, *Chem.–Asian J.*, 2021, **16**, 3805–3816.

6 C. K. Prier, D. A. Rankic and D. W. C. MacMillan, *Chem. Rev.*, 2013, **113**, 5322–5363.

7 N. A. Romero and D. A. Nicewicz, *Chem. Rev.*, 2016, **116**, 10075–10166.

8 G. Bottari, G. de la Torre, D. M. Guldi and T. Torres, *Coord. Chem. Rev.*, 2021, **428**, 213605.

9 C. G. Claessens, D. Gonzalez-Rodriguez, M. Salomé Rodriguez-Morgade, A. Medina and T. Torres, *Chem. Rev.*, 2014, **114**, 2192–2277.

10 G. de la Torre, G. Bottari and T. Torres, *Adv. Energy Mater.*, 2017, **7**, 1–21.
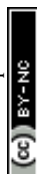
11 G. Zango, M. Krug, S. Krishna, V. Mariñas, T. Clark, M. V. Martínez-Díaz, D. M. Guldi and T. Torres, *Chem. Sci.*, 2020, **11**, 3448–3459.

12 C. G. Claessens and T. Torres, *J. Am. Chem. Soc.*, 2002, **124**, 14522–14523.

13 C. G. Claessens and T. Torres, *Chem. Commun.*, 2004, 1298–1299.

14 I. Sánchez-Molina, B. Grimm, R. M. Krick Calderon, C. G. Claessens, D. M. Guldi and T. Torres, *J. Am. Chem. Soc.*, 2013, **135**, 10503–10511.

15 T. K. Ronson, B. S. Pilgrim and J. R. Nitschke, *J. Am. Chem. Soc.*, 2016, **138**, 10417–10420.

16 W.-K. Han, H.-X. Zhang, Y. Wang, W. Liu, X. Yan, T. Li and Z.-G. Gu, *Chem. Commun.*, 2018, **54**, 12646–12649.

17 E. Fazio, C. J. E. Haynes, G. de la Torre, J. R. Nitschke and T. Torres, *Chem. Commun.*, 2018, **54**, 2651–2654.

18 C. García-Simón, A. Monferrer, M. Garcia-Borràs, I. Imaz, D. Maspoch, M. Costas and X. Ribas, *Chem. Commun.*, 2019, **55**, 798–801.

19 B. Chen, J. J. Holstein, S. Horiuchi, W. G. Hiller and G. H. Clever, *J. Am. Chem. Soc.*, 2019, **141**, 8907–8913.

20 T. A. Barendt, W. K. Myers, S. P. Cornes, M. A. Lebedeva, K. Porfyrakis, I. Marques, V. Félix and P. D. Beer, *J. Am. Chem. Soc.*, 2020, **142**, 349–364.

21 X. Chang, S. Lin, G. Wang, C. Shang, Z. Wang, K. Liu, Y. Fang and P. J. Stang, *J. Am. Chem. Soc.*, 2020, **142**, 15950–15960.

22 Y. Ni, F. Gordillo-Gámez, M. Peña Alvarez, Z. Nan, Z. Li, S. Wu, Y. Han, J. Casado and J. Wu, *J. Am. Chem. Soc.*, 2020, **142**, 12730–12742.

23 C. Fuertes-Espinosa, C. García-Simón, E. Castro, M. Costas, L. Echegoyen and X. Ribas, *Chem.– Eur. J.*, 2017, **23**, 3553–3557.

24 V. Martínez-Agramunt, T. Eder, H. Darmandeh, G. Guisado-Barrios and E. Peris, *Angew. Chem., Int. Ed.*, 2019, **58**, 5682–5686.

25 D. M. Wood, W. Meng, A. K. Ronson, A. R. Stefankiewicz, J. K. M. Sanders and J. R. Nitschke, *Angew. Chem., Int. Ed.*, 2015, **54**, 3988–3992.

26 V. Leonhardt, S. Fimmel, A.-M. Krause and F. Beuerle, *Chem. Sci.*, 2020, **11**, 8409–8415.

27 C. Fuertes-Espinosa, C. García-Simón, M. Pujals, M. Garcia-Borràs, L. Gómez, T. Parella, J. Juanhuix, I. Imaz, D. Maspoch, M. Costas and X. Ribas, *Chem*, 2020, **6**, 169–186.

28 E. Ubasart, O. Borodin, C. Fuertes-Espinosa, Y. Xu, C. García-Simón, L. Gómez, J. Juanhuix, F. Gándara, I. Imaz, D. Maspoch, M. von Delius and X. Ribas, *Nat. Chem.*, 2021, **13**, 420–427.

29 N. Huang, K. Wang, H. Drake, P. Cai, J. Pang, J. Li, S. Che, L. Huang, Q. Wang and H.-C. Zhou, *J. Am. Chem. Soc.*, 2018, **140**, 6383–6390.

30 E. Castro, A. Hernandez Garcia, G. Zavala and L. Echegoyen, *J. Mater. Chem. B*, 2017, **5**, 6523–6535.

31 Y. Katsurayama, Y. Ikabata, H. Maeda, M. Segi, H. Nakai and T. Furuyama, *Chem.– Eur. J.*, 2022, **28**, e202103223.

32 Y. Ishikawa, T. Kameyama, T. Torimoto, H. Maeda, M. Segia and T. Furuyama, *Chem. Commun.*, 2021, **57**, 13594–13597.

33 K. Matsuzaki, T. Hiromura, E. Tokunaga and N. Shibata, *ChemistryOpen*, 2017, **6**, 226–230.

34 M. D. Tzirakis and M. Orfanopoulos, *Chem. Rev.*, 2013, **113**, 5262–5321.

35 Y. Nakamura, M. Suzuki, K. Okawa, T. Konno and J. Nishimura, *J. Org. Chem.*, 2005, **70**, 8472–8477.

36 H. C. Jeong, S. H. Lim, D. W. Cho, S. H. Kim and P. S. Mariano, *Org. Biomol. Chem.*, 2016, **14**, 10502–10510.

37 S. H. Lim, J. Yi, C. S. Ra, K. Nahm, D. W. Cho, G. Y. Lee, J. Kim, U. C. Yoon and P. S. Mariano, *Tetrahedron Lett.*, 2015, **56**, 3014–3018.

38 S. H. Lim, J. Yi, G. M. Moon, C. S. Ra, K. Nahm, D. W. Cho, K. Kim, T. G. Hyung, U. C. Yoon, G. Y. Lee, S. Kim, J. Kim and P. S. Mariano, *J. Org. Chem.*, 2014, **79**, 6946–6958.

39 H. C. Jeong, S. H. Lim, Y. Sohn, Y. Il Kim, H. Jang, D. W. Cho and P. S. Mariano, *Tetrahedron Lett.*, 2017, **58**, 949–954.

40 Y. Miyake, Y. Ashida, K. Nakajima and Y. Nishibayashi, *Chem.– Eur. J.*, 2014, **20**, 6120–6125.

41 J. Y. Kim, Y. S. Lee, Y. Choi and D. H. Ryu, *ACS Catal.*, 2020, **10**, 10585–10591.

42 M. D. Tzirakis and M. Orfanopoulos, *Chem. Rev.*, 2013, **113**, 5262–5321.

43 C. Rosso, J. D. Williams, G. Filippini, M. Prato and C. O. Kappe, *Org. Lett.*, 2019, **21**, 5341–5345.

44 S. Sumino, M. Uno, T. Fukuyama, I. Ryu, M. Matsuura, A. Yamamoto and Y. Kishikawa, *J. Org. Chem.*, 2017, **82**, 5469–5474.

45 J. R. Morton, F. Negri, K. F. Preston and G. Ruel, *J. Phys. Chem.*, 1995, **99**, 10114–10117.

46 V. S. Kostromitin, A. A. Zemtsov, V. A. Kokorekin, V. V. Levin and A. D. Dilman, *Chem. Commun.*, 2021, **57**, 5219–5222.

47 Y. Xu, J. Huang, B. Gabidullin and D. L. Bryce, *Chem. Commun.*, 2018, **54**, 11041–11043.